14th International Symposium on Turbulence and Shear Flow Phenomena (TSFP14)
Heidelberg, Germany, July 28–31, 2026

DISSIMILAR DESTRUCTION OF TURBULENT MOMENTUM/HEAT FLUXES IN A MINIMAL CHANNEL FLOW

Mamoru Takahashi
Department of Mechanical Engineering
Mie University
1577 Kurimamachiya-cho, Tsu-shi, Mie, Japan
takahashi@mach.mie-u.ac.jp

Kenta Suzuki
Department of Mechanical Engineering
Mie University
1577 Kurimamachiya-cho, Tsu-shi, Mie, Japan
suzu-k@ees.mach.mie-u.ac.jp

Koichi Tsujimoto
Department of Mechanical Engineering
Mie University
1577 Kurimamachiya-cho, Tsu-shi, Mie, Japan
tujimoto@mach.mie-u.ac.jp

Toshitake Ando
Department of Mechanical Engineering
Mie University
1577 Kurimamachiya-cho, Tsu-shi, Mie, Japan
ando@mach.mie-u.ac.jp

ABSTRACT

Dissimilarity in the pressure-rate-of-strain and pressure-temperature-gradient processes, resulting in the dissimilar destruction of turbulent momentum and heat fluxes, respectively, has great potential to contribute to friction loss reduction together with heat exchange enhancement. In this study, we investigate the dissimilar destruction of turbulent fluxes in the near-wall regions of a channel flow. To capture the dissimilarity associated with self-sustaining coherent structures, such as low-speed streaks and quasi-streamwise vortices, we simulate a minimal channel flow. The dissimilar destruction events are transported from the outer to the near-wall region by the downward flows generated by quasi-streamwise vortices. This highlights the authors' previous discovery of the dissimilar destruction events in the outer region of a channel flow (Takahashi et al., Phys. Fluids, 2025). The forward- and backward-dissimilar destruction events, which reduce only the friction loss and heat exchange, tend to be separately localized downstream and upstream of the sweeping motions, respectively. The results are confirmed to be valid regardless of the self-sustaining cycle of the near-wall structures of the current minimal channel flow.

Introduction

One of the important features of turbulent flows from an engineering viewpoint is their strong exchange capability for momentum and heat. According to the Reynolds analogy, turbulent exchange of momentum and heat is similar, resulting in large heat transfer but accompanied by severe friction loss. To overcome this dilemma, researchers have investigated "dissimilar" exchange phenomena generated by several external control inputs (Inaoka *et al.*, 1999; Hasegawa & Kasagi, 2011; Kaithakkal *et al.*, 2020; Yamamoto *et al.*, 2022) or even in non-Newtonian fluid flows (Hara *et al.*, 2023).

It is widely believed that the Reynolds analogy is governed by coherent structures that exchange momentum and heat simultaneously. Accordingly, the physics associated with these coherent structures has generally been investigated to improve our understanding of turbulent transport phenomena. However, despite the long history of turbulence research, no coherent eddy structure has been identified that exchanges only heat, implying the difficulty of breaking the Reynolds analogy by controlling the well-known structures. In contrast, the destruction processes of turbulent momentum and heat fluxes have been much less investigated. This suggests the possible existence of undiscovered "dissimilar destruction events of turbulent fluxes," which cause a loss of turbulent momentum flux accompanied by a gain of turbulent heat flux, and which may contribute to friction reduction together with heat-transfer enhancement.

Because turbulent momentum and heat fluxes are anisotropic statistical quantities, they are reduced through the so-called "return-to-isotropy" process. Accordingly, the principal sink terms in the transport equations for the turbulent momentum and heat fluxes are the pressure–strain-rate and pressure–temperature-gradient terms, respectively:

$$\Phi_{uv} \equiv \overline{p'\left(\frac{\partial v'}{\partial x}+\frac{\partial u'}{\partial y}\right)}, \quad (1)$$

$$\Phi_{v\theta} \equiv \overline{p'\frac{\partial \theta'}{\partial y}}. \quad (2)$$

Based on this idea, the authors recently identified local flow patterns associated with the dissimilar destruction mechanisms of turbulent fluxes in an uncontrolled channel flow (Takahashi *et al.*, 2025). The main finding was that the loss of momentum flux and the gain of heat flux occur simultaneously when vertically sheared flows are rolled up by spanwise swirling motions. However, although such flow patterns were detected away from the wall ($y^+ \sim 100$, where $^+$ denotes normalization using viscous scales), because the similarity constraint imposed by the boundaries weakens with increasing distance from the wall, a large portion of the turbulent exchange of momentum and heat takes place in the near-wall region ($y^+ \sim 10$).

In this study, we capture dissimilar destruction events in the near-wall region of a channel flow. Special attention is paid to the relationship between the formation of these dissimilar

Table 1. Numerical parameters

Re_τ	$(L_x/h, L_z/h)$	(L_x^+, L_z^+)	(N_x, N_y, N_z)
200	$(1.8, 0.6)$	$(353, 116)$	$32, 128, 16$

destruction events and well-known coherent structures, such as low-speed streaks and quasi-streamwise vortices. To sustain only a minimal number of such structures in the numerical domain, we simulate a "minimal channel flow" (Jiménez & Moin, 1991), which consists of a single pair of low- and high-speed streaks. Accordingly, we also examine the generation of dissimilar destruction events within the self-sustaining cycle of the simulated flow system.

Numerical techniques

The velocity and temperature fields are governed by the continuity equation, Navier–Stokes equation, and advection–diffusion equation:

$$\frac{\partial u_i}{\partial x_i} = 0, \tag{3}$$

$$\frac{\partial u_i}{\partial t} + u_j \frac{\partial u_i}{\partial x_j} = -\frac{\partial p}{\partial x_i} + \frac{1}{\mathrm{Re}} \frac{\partial^2 u_i}{\partial x_j \partial x_j}, \tag{4}$$

$$\frac{\partial \theta}{\partial t} + u_i \frac{\partial \theta}{\partial x_i} = Q_\theta + \frac{1}{\mathrm{RePr}} \frac{\partial^2 \theta}{\partial x_i \partial x_i}, \tag{5}$$

where u_i is the instantaneous velocity in the x_i direction [$i = 1$, 2, 3, $(x_1, x_2, x_3) = (x, y, z)$, $(u_1, u_2, u_3) = (u, v, w)$], p is the pressure per unit mass, Re is the balk Reynolds number (using the channel half-width h), Pr is the Prandtl number, θ is the temperature, and Q_θ is the bulk heat source. The time integration of the governing equations uses the fourth-order Runge–Kutta method. The spatial numerical derivative is obtained from a second-order central finite difference scheme.

The simulations employ periodic boundary conditions along the streamwise and spanwise directions, and zero-velocity/-temperature conditions at the walls. In addition, we assign $Q_\theta = -\partial \overline{p}/\partial x$ and the Prandtl number $\mathrm{Pr} = 1$. Thus, the primitive difference between the fluctuating streamwise velocity and the temperature is only the presence or absence of the fluctuating pressure gradient. Such boundary and driving conditions were also employed in the previous studies on the dissimilar momentum/heat exchange control in channel flows (Hasegawa & Kasagi, 2011; Yamamoto *et al.*, 2022).

The friction Reynolds number $\mathrm{Re}_\tau \equiv u_\tau h/\nu$, the streamwise and spanwise lengths of the numerical domain, L_x and L_z/h, respectively, and the grid numbers in the three directions are summarized in Table 1. This setup is confirmed to be sufficient as the minimal flow unit to sustain the self-sustaining near-wall structures.

Figure 1(a) and (b) show the budgets of the turbulent momentum and heat fluxes, respectively. Although not shown here, we confirmed that the lower-order statistics, such as the mean and root-mean-square values of the streamwise velocity and temperature, are in good agreement with the reference data (Jiménez & Moin, 1991). The present results are compared with the reference data (Takahashi *et al.*, 2025), which were obtained from a channel flow with a larger computational domain. Despite the qualitative agreement with the reference data in the near-wall region, some quantitative discrepancies are observed, possibly owing to the minimal computational setup, which limits non-local (spatial) interactions between the near- and outer-wall structures.

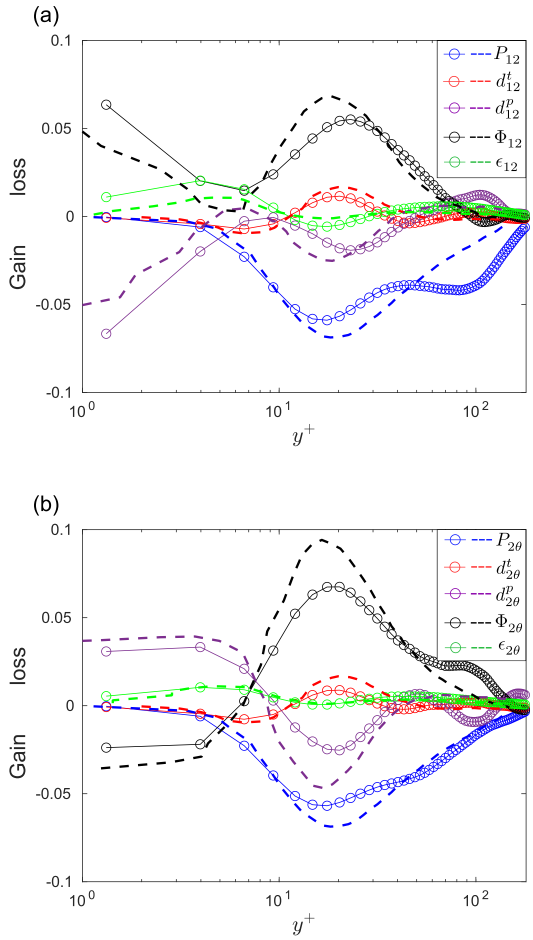

Figure 1. Budget of (a) turbulent momentum flux and (b) turbulent heat flux. Circles with solid lines, current Minimal flow; thick dashed lines, full-size channel flow Takahashi *et al.* (2025). Blue, production; black, destruction; red, turbulent diffusion; purple, pressure diffusion; green, dissipation.

Dissimilarity in turbulent flux destruction during self-sustaining periodic cycle

Consider instantaneous events satisfying

$$\Phi'_{uv} \equiv p'\left(\frac{\partial v'}{\partial x} + \frac{\partial u'}{\partial y}\right) > 0 \cap \Phi'_{v\theta} \equiv p'\frac{\partial \theta'}{\partial y} < 0, \tag{6}$$

or, conversely,

$$\Phi'_{uv} \equiv p'\left(\frac{\partial v'}{\partial x} + \frac{\partial u'}{\partial y}\right) < 0 \cap \Phi'_{v\theta} \equiv p'\frac{\partial \theta'}{\partial y} > 0, \tag{7}$$

that is, events that simultaneously contribute to the loss of turbulent momentum flux ($D\overline{u'v'}/Dt > 0$) and the gain of turbulent heat flux ($D\overline{v'\theta'}/Dt < 0$), or vice versa. We refer to

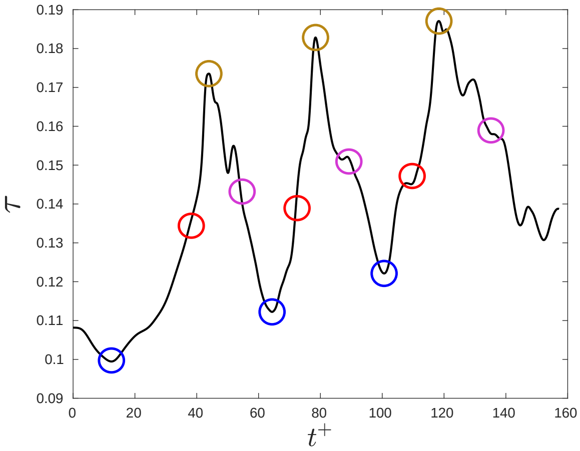

Figure 2. Evolution of planar-averaged wall-shear stress. The minimal channel flow is characterized by the four types of phases in the cyclical variation: “Trough”, “Ascending”, “Peak”, and “Descending”.

the former and latter as “forward-dissimilar” and “backward-dissimilar” destruction events, respectively.

Figure 2 shows the temporal evolution of the planar-averaged wall-shear stress $\tau \equiv (1/L_x L_z) \int \nu (\partial u/\partial y)|_{y=0}\, dx dz$. The cyclic variation of τ confirms the self-sustaining process of coherent motions in the minimal channel flow. We characterize this cycle by four distinct phases: “Trough”, “Ascending”, “Peak”, and “Descending”. As reported in many previous studies on the self-sustaining mechanism of near-wall coherent structures (Hamilton *et al.*, 1995; Waleffe, 1997), quasi-streamwise vortices generate low-speed streaks in the trough phase; the streaks subsequently break down owing to instability, thereby intensifying turbulence; the turbulence then weakens, while nonlinear interactions regenerate the quasi-streamwise vortices.

Representative momentum and heat transfer associated with quasi-streamwise vortices in the four phases are illustrated in Fig. 3. The right panels show instantaneous cross-stream velocity distributions on y–z planes intersecting prominent dissimilar destruction events. The velocity vectors clearly capture the swirling motions of the quasi-streamwise vortices. As indicated in Fig. 2, turbulence is strongest in the “Peak” phase, weakest in the “Trough” phase, and intermediate in the “Ascending” and “Descending” phases.

Throughout the four phases, both forward- and backward-dissimilar events are predominantly localized in the downstream regions between two counter-rotating vortices; for example, at $z^+ \sim 10$ in the “Trough”, 40 in the “Ascending”, 90 in the “Peak”, and 40 in the “Descending”. In particular, at $z^+ \sim 90$ in the “Peak” phase and 40 in the “Descending” phase, the instantaneous turbulent heat flux $v'\theta'$ exceeds its momentum-flux counterpart $u'v'$, demonstrating the significant contribution of the dissimilar destruction events to friction-loss reduction accompanied by enhanced heat transfer. In contrast, in the upstream regions associated with the low-speed streaks (indicated by the local peaks of the cyan dashed lines), the distributions of $u'v'$ and $v'\theta'$ are highly similar; for example, at $z^+ \sim 80$ in the “Ascending”, 50 in the “Peak”, and 90 in the “Descending”. This similarity is expected because the momentum and temperature fields in the near-wall fluid are constrained by the wall boundary conditions. In other words, the breakdown of the Reynolds analogy associated with dissimilar turbulent-flux destruction is first generated in the outer region and subsequently transported toward the near-wall region by coherent eddies. This highlights the impact of the dissimilar destruction events previously identified by the authors (Takahashi *et al.*, 2025), although they were detected primarily in the outer region ($y^+ \sim 100$).

Therefore, we next investigate the phase-averaged concentration of forward- and backward-dissimilar destruction events around “sweep” motions ($u' > 0 \cap v' < 0$). Each instantaneous flow field is horizontally shifted so that the location of the maximum sweep event coincides with the center of the numerical domain. Hereafter, phase-averaged quantities are denoted by hats, for example, $\widehat{u'}$.

The left panel in Fig. 4 shows the phase-averaged wall-shear stress as a function of phase. Letting φ denote the phase and T the “Trough-to-Trough” period, the “Trough”, “Ascending”, “Peak”, and “Descending” phases correspond to $\varphi/T =$ 0, 0.25, 0.5, and 0.75, respectively. The right panels show the x^+–y^+ planar distributions of the phase-averaged streamwise velocity $\widehat{u'^+}$ and the dissimilar turbulent momentum-flux destruction $\widehat{\Phi'^+_{uv}}$ at $z^+ = 58$. Owing to the horizontal alignment of the flow fields, the peaks of $\widehat{u'^+}$ appear at the center of the numerical domain. The peak magnitudes are nearly identical across the four phases, indicating that the locally transferred momentum from the outer region is largely independent of the near-wall cycle. Moreover, the locations and intensities of the forward- and backward-dissimilar destruction events remain consistent throughout the four phases. The self-sustaining process appears to modulate only the probability that these dissimilar destruction events are transported from the outer region toward the near-wall region by quasi-streamwise vortices.

This finding indicates that the formation of the dissimilar destruction events is largely independent of the quasi-periodic near-wall cycle and is instead governed by dynamics originating in the outer region. Although our previous study (Takahashi *et al.*, 2025) focused on phenomena identified away from the wall, the present results demonstrate that the near-wall manifestations are primarily a consequence of their transport from the outer layer. This not only alleviates concerns regarding the wall-normal relevance, but also reinforces the impact of the previous discovery on turbulent momentum and heat transfer.

Furthermore, the forward-dissimilar destruction events are predominantly localized downstream of the sweep motions, whereas the backward-dissimilar events are localized upstream. This spatial separation suggests the potential for developing turbulence-control strategies based on the dissimilar destruction of turbulent fluxes: if the concentration locations of the forward- and backward-dissimilar destruction events were to coincide, selectively enhancing the forward-dissimilar events while suppressing the backward-dissimilar ones would be considerably more difficult. This interpretation is further supported by the all-phase-averaged (i.e., unconditioned) concentration of the forward- and backward-dissimilar destruction events shown in Fig. 5. The results more clearly demonstrate the symmetry of the concentration locations of the dissimilar destruction events with respect to the sweep motions.

Conclusions

The dissimilar destruction events observed in the near-wall region are preferentially located between neighboring quasi-streamwise vortices. Combined with our previous findings, this indicates that these destruction events are not generated locally at the wall, but instead originate in the outer region—where direct boundary effects are weak—and are sub-

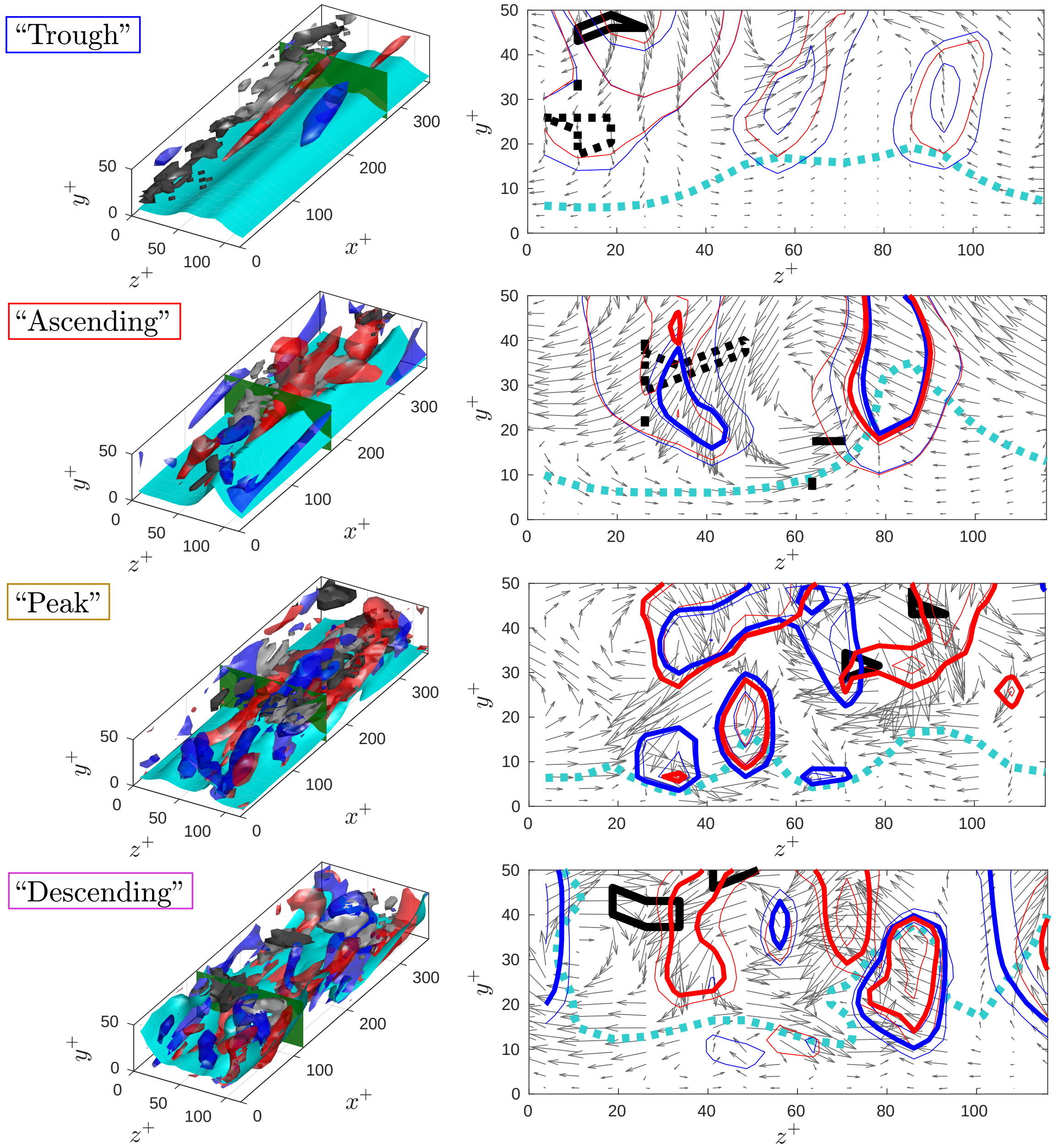

Figure 3. Representative momentum and heat transfer associated with quasi-streamwise vortices. The blue and red isosurfaces denote $Q = 0.22\max(Q)$ (blue: $\omega_x > 0$; red: $\omega_x < 0$), and the cyan isosurface denotes $u = U|_{y^+=24}$, illustrating the quasi-streamwise vortices and the low-speed streak. The dark- and light-gray isosurfaces correspond to $\Phi_{u'v'} = 0.5\max(\Phi_{u'v'})$, representing the forward- and backward-dissimilar destruction events, respectively. The right panels display velocity vectors on the cross-sectional plane shown in the left panels (green transparent planes). The blue and red contours indicate the instantaneous momentum flux $u'v'$ and heat flux $v'\theta'$, respectively. The thick solid and dashed lines again represent the forward- and backward-dissimilar events, respectively, shown as contours of $\Phi_{u'v'} = 0.5\max(\Phi_{u'v'})$.

sequently transported toward the wall by the downward motions induced by the quasi-streamwise vortices. In contrast, the turbulent momentum and heat fluxes themselves, as well as their destruction processes within the low-speed streaks, exhibit strong similarity due to the imposed boundary conditions. These results highlight the intrinsic non-locality of turbulent momentum and heat transport in wall-bounded turbulence and demonstrate that the dissimilar destruction events arise from interactions between outer-layer dynamics and near-wall coherent structures. The present minimal-unit analysis thus reinforces the outer-layer origin of the phenomenon, while requires further examination using regular channel flows with larger computational domains for quantitative assessment and broader generalization.

Furthermore, the spatial organization of the destruction events exhibits a clear symmetry relative to intense sweep motions: forward-dissimilar destruction events are localized downstream, whereas backward-dissimilar events are concentrated upstream. This separation suggests a potential pathway for turbulence control based on selectively manipulating the dissimilar destruction of turbulent fluxes. In particular, the results point toward strategies for simultaneous friction reduction and heat-transfer enhancement through actuation that promotes forward-dissimilar destruction events in the outer region

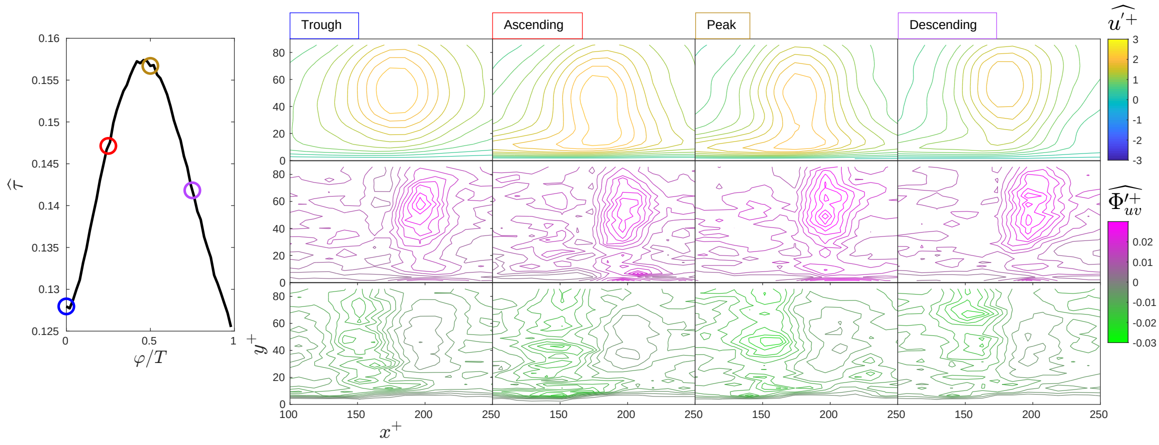

Figure 4. (Left) Phase-averaged wall-shear stress as a function of phase. The four characteristic phases (“Trough”, “Ascending”, “Peak”, and “Descending”) are indicated by open-circle symbols. (Right) x^+–y^+ planar distributions at $z^+ = 58$ of phase-averaged streamwise velocity $\widehat{u'^+}$ (top), forward-dissimilar turbulent momentum-flux destruction $\widehat{\Phi'^+_{uv}}$ (middle), and backward-dissimilar turbulent momentum-flux destruction $\widehat{\Phi'^+_{uv}}$ (bottom).

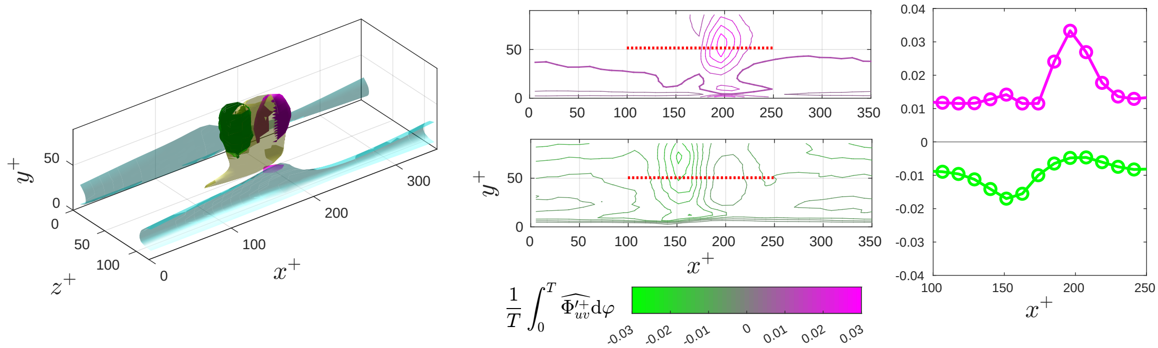

Figure 5. (Left) Isosurfaces of all-phase-averaged streamwise velocity (yellow and cyan for positive and negative values, respectively) and dissimilar destruction events (magenta and green for forward- and backward-dissimilar events, respectively). (Middle) x^+–y^+ planar distributions of all-phase-averaged dissimilar destruction events at $z^+ = 58$: forward-dissimilar destruction (top) and backward-dissimilar destruction (bottom). (Right) One-dimensional distributions of all-phase-averaged forward- (top) and backward-dissimilar destruction (bottom) along the red dashed line shown in the middle panels.

or downstream of strong sweep motions.

Note that, since the present flow is uncontrolled and developed over smooth walls, the probability and intensity of the forward- and backward-dissimilar destruction events are comparable, leading to substantial mutual cancellation. Nevertheless, the identification of their spatial organization and transport mechanisms under such restrictive conditions highlights the intrinsic robustness of the phenomenon. Although effective strategies for selectively amplifying or suppressing these paired events remain to be established, the present results implies that turbulence control based on dissimilar destruction is, at least in principle, feasible.

REFERENCES

Hamilton, J., Kim, J. & Waleffe, F. 1995 Regeneration mechanisms of near-wall turbulence structures. *Journal of Fluid Mechanics* **287**, 317–348.

Hara, Shumpei, Watanabe, Kana, Kaiho, Yuichi, Tsukahara, Takahiro & Kawaguchi, Yasuo 2023 Dissimilar turbulent momentum and heat transfer associated with viscoelastic vibration in channel flow. *International journal of heat and mass transfer* **207**, 123991.

Hasegawa, Y & Kasagi, N 2011 Dissimilar control of momentum and heat transfer in a fully developed turbulent channel flow. *Journal of fluid mechanics* **683**, 57–93.

Inaoka, K, Yamamoto, J & Suzuki, K 1999 Dissimilarity between heat transfer and momentum transfer in a disturbed turbulent boundary layer with insertion of a rod – modeling and numerical simulation. *International Journal of Heat and Fluid Flow* **20** (3), 290–301.

Jiménez, Javier & Moin, Parviz 1991 The minimal flow unit in near-wall turbulence. *Journal of fluid mechanics* **225** (-1), 213–240.

Kaithakkal, Arjun J, Kametani, Yukinori & Hasegawa, Yosuke 2020 Dissimilarity between turbulent heat and momentum transfer induced by a streamwise travelling wave of wall blowing and suction. *Journal of fluid mechanics* **886**, A29.

Takahashi, M, Inagaki, Y, Tsujimoto, K & Ando, T 2025 Similar and dissimilar destruction of turbulent fluxes in a low-reynolds-number channel flow. *Physics of fluids (Woodbury, N.Y.: 1994)* **37** (1), 015107.

Waleffe, F. 1997 On a self-sustaining process in shear flows. *Physics of Fluid* **9**, 883–900.

Yamamoto, R, Morita, J, Mamori, H, Miyazaki, T & Hara, S 2022 Turbulent channel flow controlled by traveling-wave-like body force mimicking oscillating thin films. *Physics of fluids* **34** (8).